Analysis of Phosphorescence in Heterogeneous Systems Using Distributions of Quencher Concentration

Aleksander S. Golub, Aleksander S. Popel,* Lei Zheng, and Roland N. Pittman
Department of Physiology, Medical College of Virginia, Virginia Commonwealth University, Richmond, Virginia 23298-0551, and
*Department of Biomedical Engineering, School of Medicine, Johns Hopkins University, Baltimore, Maryland 21205 USA

ABSTRACT A continuous distribution approach, instead of the traditional mono- and multiexponential analysis, for determining quencher concentration in a heterogeneous system has been developed. A mathematical model of phosphorescence decay inside a volume with homogeneous concentration of phosphor and heterogeneous concentration of quencher was formulated to obtain pulse-response fitting functions for four different distributions of quencher concentration: rectangular, normal (Gaussian), gamma, and multimodal. The analysis was applied to parameter estimates of a heterogeneous distribution of oxygen tension (PO_2) within a volume. Simulated phosphorescence decay data were randomly generated for different distributions and heterogeneity of PO_2 inside the excitation/emission volume, consisting of 200 domains, and then fit with equations developed for the four models. Analysis using a monoexponential fit yielded a systematic error (underestimate) in mean PO_2 that increased with the degree of heterogeneity. The fitting procedures based on the continuous distribution approach returned more accurate values for parameters of the generated PO_2 distribution than did the monoexponential fit. The parameters of the fit (M = mean; σ = standard deviation) were investigated as a function of signal-to-noise ratio (SNR = maximum signal amplitude/peak-to-peak noise). The best-fit parameter values were stable when SNR $\geq$ 20. All four fitting models returned accurate values of M and σ for different PO_2 distributions. The ability of our procedures to resolve two different heterogeneous compartments was also demonstrated using a bimodal fitting model. An approximate scheme was formulated to allow calculation of the first moments of a spatial distribution of quencher without specifying the distribution. In addition, a procedure for the recovery of a histogram, representing the quencher concentration distribution, was developed and successfully tested.

INTRODUCTION

Measurement of the concentration of some substances by their ability to quench the phosphorescence of excited phosphors has become a precise, noninvasive method in biological studies (Vanderkooi et al., 1987; Wilson et al., 1991; Shonat et al., 1992, 1995; Torres Filho and Intaglietta, 1993; Torres Filho et al., 1994, 1996; Kerger et al., 1995, 1996; Zheng et al., 1996). In homogeneous systems (i.e., media with constant phosphor and quencher concentrations) a simple application of the Stern-Volmer equation to determine quencher concentration from phosphorescence lifetime yields reliable results. In microcirculatory measurements of oxygen concentration in relatively large arterioles and venules reported by Torres Filho et al. (Torres Filho and Intaglietta, 1993; Torres Filho et al., 1996), and in in vitro determinations of oxygen consumption by mitochondria reported by Wilson et al. (1991), the heterogeneity in quencher concentration was assumed to be negligible, and the phosphorescence decay curves were analyzed in terms of a monoexponential time course.

Large nonuniformities of quencher concentration in biological systems (e.g., oxygen in the microcirculation: Ellsworth and Pittman, 1986; Ellsworth et al., 1988; Kuo and Pittman, 1988, 1990; Popel, 1989; Swain and Pittman, 1989) present a considerable difficulty in the application of the phosphorescence quenching technique. It is generally accepted that the phosphorescence decay time course in a heterogeneous system consists of several exponentials (Siemiarczuk et al., 1990; Ware, 1991; Vinogradov and Wilson, 1994), and that one can decompose the phosphorescence decay curve into an arbitrary number of additive exponential terms. However, the existence of a good statistical fit by a given set of exponentials does not necessarily imply that these exponential terms correspond to the actual phosphorescence decays within the various spatial domains of the excitation volume.

Useful experience in the analysis of complex decay curves has been acquired in a number of different research areas. There are several types of problems in which the data can be represented by an integral over an exponential kernel (Provencher, 1976a,b):

$$y(t) = \int_0^\infty \exp(-\lambda t) f(\lambda)\, d\lambda \qquad (1)$$

The goal of the analysis of these problems is to determine the spectrum, $f(\lambda)$, from a finite data set, $y(t)$. In many applications, such as the analysis of multicomponent radioactive decay curves, the spectrum is discrete and the integral in Eq. 1 can be represented as a linear combination of

Received for publication 19 August 1996 and in final form 10 April 1997.

Address reprint requests to Dr. Roland N. Pittman, Department of Physiology, P.O. Box 980551, Medical College of Virginia, Virginia Commonwealth University, Richmond, VA 23298-0551. Tel.: 804-828-9545; Fax: 804-828-7382; E-mail: pittman@gems.vcu.edu.

0006-3495/97/07/452/14 $2.00

exponentials (Gardner et al., 1959):

$$y(t) = \sum_{i=1,n} w_i \exp(-\lambda_i t) \quad (2)$$

In this situation, the n lifetimes, λ_i, and $n - 1$ preexponential factors, w_i, must be determined from the normalized data set, where $y(0) = 1$ and $\Sigma_{i=1,n} w_i = 1$.

The analysis of fluorescence decay curves in pulse fluorimetry is the problem most closely related to that of heterogeneous phosphorescence considered in the present paper. It was found that most protein and nucleic acid conjugates have multicomponent fluorescent decays due to the heterogeneity of chromophores and bound ligands (Isenberg and Dyson, 1969). It was assumed that the spectrum was discrete, with four or fewer components (Gardner et al., 1959; Isenberg and Dyson, 1969; Ware et al., 1973; Provencher, 1976a,b; Lakowicz et al., 1984). Attempts to resolve the discrete components of the decay curves fall into several categories (Isenberg and Dyson, 1969): repeated subtraction of the slowest decays on a semilog plot; a curve-fitting procedure; and the "method of moments." Fourier transforms, inverse Laplace transforms, eigenfunction expansions, and least-square methods are other approaches that have been proposed and used for the deconvolution of Eq. 2 (Gardner et al., 1959; Isenberg and Dyson, 1969; Ware et al., 1973; Provencher, 1976a,b). The analysis of lifetimes from phase fluorometry data was also based on the assumption of a discrete spectrum (Lakowicz et al., 1984). Further investigations showed that, despite the capacity of two- or three-exponential terms to provide good fits of the data, the recovered parameters provided little information about the underlying continuous distributions of lifetimes (James and Ware, 1985). However, for mono- and bimodal Gaussian distributions of lifetimes, the two-exponential model was found to be a useful approximation (James et al., 1985).

An understanding of the continuous nature of the lifetime distribution led to the development of the exponential series method (ESM), in which a multiexponential fitting function with fixed lifetimes and variable preexponential coefficients was used (James and Ware, 1986). Because this method uses fixed lifetimes that uniformly span the range of the underlying distribution, the number of recovered parameters is $n - 1$ instead of $2n - 1$. Although the resulting problem is a linear one, the nonlinear Marquardt algorithm or other fitting procedure that can constrain the preexponentials to positive values is needed for analysis. Another powerful analytical technique, the maximum entropy method (MEM), can successfully handle the inverse Laplace transforms of decay curves (Livesey and Brochon, 1987). A reconstructed spectrum using this method consists of a large number of discrete lines with amplitude w_i, equally spaced in $\log(1/\lambda_i)$. The two methods (ESM and MEM) are similar in their resolving power, and both can handle up to 200 exponential terms in the fitting function (Siemiarczuk et al., 1990, 1993). Vinogradov and Wilson (1994) have recently developed a quadratic programming algorithm to algebraically decompose the phosphorescence decay curve into a linearly independent set of 200 exponentials. The common point in these methods is the recovery of a continuous distribution with a set of exponentials having regularly spaced and fixed lifetimes. It has been shown that a discrete distribution with a high density of components gives the same result as a continuous distribution. Unfortunately, a large number of fitting parameters, arising from the discrete representation of the continuous lifetime distribution, leads to a relatively long computation time, a high sensitivity to noise, and uncertainties in the results because of the large number of degrees of freedom. Furthermore, attainment of a high signal-to-noise ratio necessitates averaging many decay curves. These features make it less practical for on-line measurements in biological systems like microvessels, especially when non-steady-state gradients in quencher concentration are present.

In the microscopic measurement of single microvessels and cells, the phosphorescence signal is weak because of the small volume of excitation (and emission) and the low concentration of phosphor in the blood plasma or cytoplasm, limited for considerations of constant tonicity and low toxicity. Moreover, because the conditions inside the excitation volume of a microvessel or cell can vary significantly in time, the common practice of averaging a sequence of decay curves cannot be followed. Furthermore, the phosphorescence decay signal from the microvolume with a gradient in quencher concentration should contain information about the quencher heterogeneity that could be extracted by analysis with an appropriately formulated physical model. An example of quencher heterogeneity is the nonuniform partial pressure of oxygen inside microvascular plasma that is created by diffusion gradients.

A fruitful approach for the recovery of a continuous distribution was presented by Alcala et al. (1987) in the context of computer simulations of data obtained from phase fluorometry. They proposed the use of a probability density function and its combinations to recover the underlying distributions. The uniform (rectangular) distribution was found to be a good model for several different lifetime distributions. It was also concluded that the analysis of data in terms of probability density and lifetime distribution functions was less sensitive to systematic errors due to the weighting of the data. These findings could be applied to the analysis of pulse phosphorescence data in terms of a continuous distribution of quencher concentration.

In the present work we develop a continuum approach for the interpretation of pulse response functions obtained from heterogeneous phosphorescent systems containing a gradient in quencher concentration. In our description, we use a formalism from the theory of probability and statistics. However, the similarity may end there because, for a single excitation experiment, the spatial distribution of quencher is deterministic. Because the aim of recovering the underlying distribution is to find an appropriate descriptive statistical

model and express it in terms of statistical moments, we will seek relationships between the underlying distribution and the shape of the phosphorescence decay curve. Such a result can be obtained by using the Laplace transform of probability density functions as fitting models and their moments as fitting parameters. This approach will allow the use of nonlinear fitting procedures to determine the moments of the underlying distribution and to choose an adequate distribution using standard best-fit criteria.

We propose to use a continuous distribution of quencher concentration characterized by several parameters of the fitting function. We will seek the parameters of the distribution of quencher concentration instead of the distribution of lifetimes, allowing the direct Laplace transform of a continuous distribution to be used instead of the inverted Laplace transform of the phosphorescence decay curve. The Laplace transform of the continuous distribution of quencher concentration will be used as a fitting function instead of a sum of exponentials. We will apply the concept of a rectangular distribution to develop a procedure for recovery of the histogram representing a continuous distribution.

MATHEMATICAL MODEL

Phosphorescence in a homogeneous system

The phosphorescence quenching technique is based on the two modes of deactivation of excited phosphor molecules. After photoexcitation, the concentration of excited phosphor molecules is reduced by light emission from the excited state (i.e., phosphorescence emission) and by energy transfer to quencher molecules (oxygen is the only quencher in physiological systems such as blood; Vinogradov et al., 1996). The rate of change of concentration of the excited phosphor molecules after their excitation at $t = 0$ is given by

$$dN/dt = -k_0N - k_qNQ \tag{3}$$

where $N(t)$ is the concentration of excited phosphor molecules at time t, k_0 is the first-order rate constant for phosphorescent decay in the absence of quencher, k_q is the second-order rate constant in the presence of quencher, and Q is the quencher concentration. The first term in this equation represents the rate of deactivation due to light emission, and the second term represents the rate of deactivation due to quenching. The constant $k_0 = 1/\tau_0$, where τ_0 is the lifetime of phosphorescence decay when $Q = 0$. The solution of Eq. 3 is

$$N(Q, t) = N_0\exp(-k_0 + k_qQ)t) \tag{4}$$

where N_0 is the initial value of excited phosphor concentration. Light intensity, $I(t)$, is proportional to the rate of phosphor deactivation by light emission (Eq. 1) and, consequently, to the concentration of excited phosphor molecules; thus

$$I(Q, t) = I_0\exp(-(k_0 + k_qQ)t) = I_0\exp(-t/\tau) \tag{5}$$

where I_0 is the initial value of light intensity per unit volume and τ is the phosphorescence decay lifetime in the presence of the quencher. This equation can be written as

$$Y_M(Q, t) = I(Q, t)/I_0 = \exp(-(k_0 + k_qQ)t) = \exp(-t/\tau) \tag{6}$$

where $Y_M(Q, t)$ is the normalized photometric signal from the emission volume with homogeneous concentration distribution (monoexponential model). The Stern-Volmer equation that relates phosphorescence lifetime, τ, to quencher concentration, Q, can be written as

$$1/\tau = 1/\tau_0 + k_qQ \tag{7}$$

Phosphorescence in a heterogeneous system

Consider a system containing a phosphorescent probe of homogeneous concentration, but a quencher of heterogeneous concentration. Let us assume that, at time $t = 0$, a flash of light of infinitesimally short duration produces a uniform concentration, N_0, of excited phosphor molecules. The time scale for flash duration and phosphorescence lifetime together is assumed to be short enough that mass transfer by diffusion and convection can be neglected. Within the excitation volume, V, the quencher concentration ranges from Q_{min} to Q_{max}. In principle, V could be subdivided into infinitesimal homogeneous volumes, each associated with a particular value of Q and corresponding monoexponential phosphorescence decay with lifetime given by Eq. 7. For the purpose of analyzing the phosphorescence signal from V, domains of equal Q are combined, even if they are not contiguous within V. Next, all of the smaller volumes are arranged by increasing values of Q and normalized to the whole volume. The distribution function $f(Q)$ is defined so that $f(Q)dQ$ is equal to the fractional volume dV/V, in which the values of the quencher concentration vary between Q and $Q + dQ$. Thus $f(Q)$ characterizes the distribution of quencher concentration in the excitation volume (see Fig. 1). The distribution function, $f(Q)$, obeys the normalization condition

$$\int_{Q_{min}}^{Q_{max}} f(Q)\, dQ = 1 \tag{8}$$

and is similar to a probability density function, although in this case the function characterizes not a random process, but a deterministic distribution of Q. For convenience, we can extend the definition of the distribution function: $f(Q) = 0$ for $0 \le Q < Q_{min}$ and $Q > Q_{max}$. Then the integral in Eq. 8 can be calculated over the range from 0 to ∞. Using this distribution function, the mean (M) and variance (σ^2) of

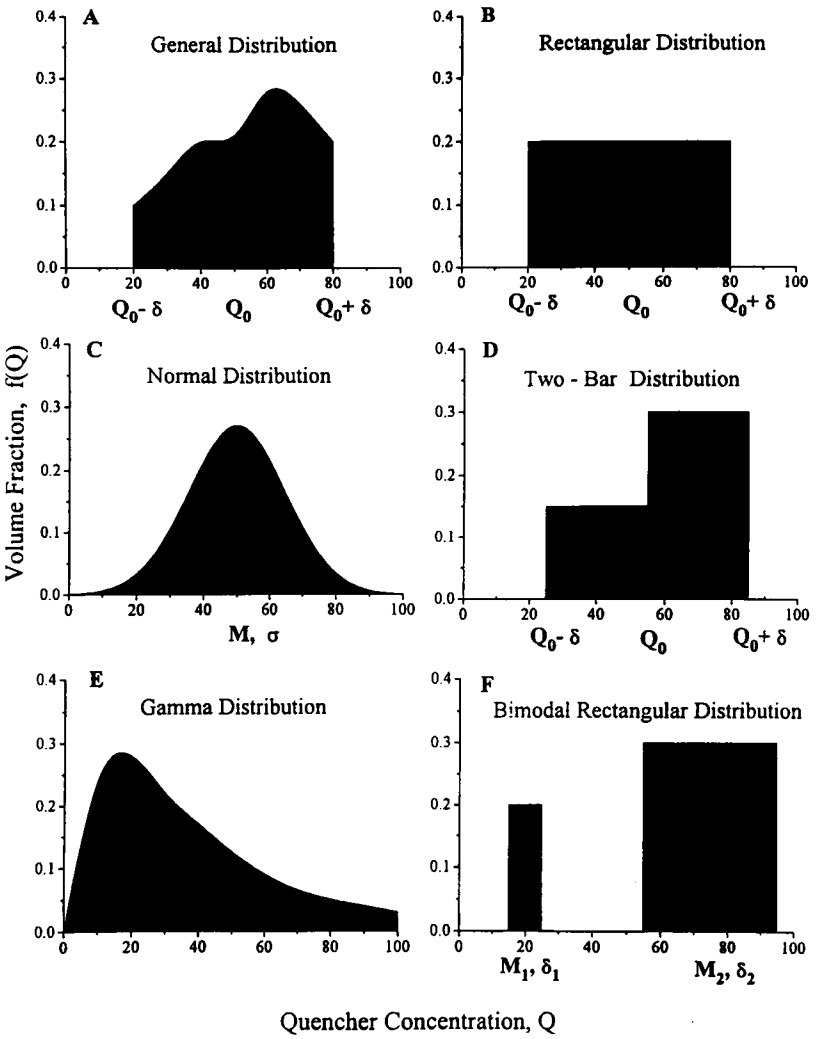

FIGURE 1 Examples of continuous distributions of quencher concentration. Fractional volume, $v(Q)$, is plotted on the ordinate, and quencher concentration, Q, is plotted on the abscissa. These examples are described in more detail in the text.

Q in the volume can be calculated as

$$M = \int_0^\infty Qf(Q)\,dQ \tag{9}$$

$$\sigma^2 = \int_0^\infty (Q - M)^2 f(Q)\,dQ \tag{10}$$

Higher order central moments that will be used below are calculated as

$$\mu_n = \int_0^\infty (Q - M)^n f(Q)\,dQ \tag{11}$$

Thus $\mu_2 = \sigma^2$; $\gamma_1 = \mu_3/\sigma^3$ is known as the skewness or asymmetry coefficient; and $\gamma_2 = \mu_4/\sigma^4 - 3$ is known as the kurtosis or excess coefficient.

Because of optical limitations, it is not possible to collect the total light yield from the emission volume using conventional microscopy. We can avoid dealing with absolute values of the signal intensity by normalizing the photometric signal. We recast Eq. 6 in the form

$$Y(t) = I(t)/I_0 = \int_0^\infty \exp(-(k_0 + k_q Q)t) f(Q)\,dQ \tag{12}$$

The normalized function $Y(t)$ is obtained experimentally, and the coefficients k_0 and k_q can be determined by calibration (in vitro or in vivo). Therefore the task of interpreting the phosphorescence decay curve is reduced to determining the quencher distribution function, $f(Q)$, in the emission volume.

For a continuous distribution $f(Q)$, Eq. 12 is an integral Fredholm equation of the first kind (Morse and Feshbach, 1953). Alternatively, Eq. 12 can be rewritten in the form

$$F(s) = Y(t)\exp(k_0 t) = \int_0^\infty \exp(-sQ) f(Q)\,dQ \tag{13}$$

where $s = k_q t$, and therefore the right-hand side of Eq. 13 can be considered as the Laplace transform of $f(Q)$ (Boas, 1983).

Some properties of the Laplace transform that show an intrinsic relationship between the moments of quencher distribution and the shape of the decay time course are

1. The integral of the quencher distribution function is equal to the initial value of $F(s)$ when $s \rightarrow 0$; this can be expressed in the form

$$Y(0) = \int_0^\infty f(Q)\, dQ = 1 \tag{14}$$

because $f(Q)$ is normalized according to Eq. 8.

2. The negative derivative of $F(s)$ as $s \rightarrow 0$ is equal to the first moment of the quencher distribution function describing the quencher concentration; this property can be expressed as

$$dY/dt|_{t\rightarrow 0} = -(k_0 + k_q M) \tag{15}$$

3. The second derivative of $F(s)$ as $s \rightarrow 0$ is equal to the ordinary (i.e., not central) second moment (σ_0^2) of the quencher distribution function; this result can be expressed as

$$d^2Y/dt^2|_{t\rightarrow 0} = (k_0 + k_q M)^2 + (k_q \sigma_0)^2 \tag{16}$$

Consequently, the phosphorescence decay curve obtained from a heterogeneous system contains information on the moments of the distribution function that can be estimated by appropriate mathematical procedures.

The property of linearity will be used in the development of a procedure for recovering the histogram that describes a multimodal distribution. The Laplace transform of a sum of functions, $f_i(Q)$, each weighted by a coefficient, w_i, is equal to the sum of the Laplace transforms:

$$\int_0^\infty \exp(-sQ) \sum_i w_i f_i(Q)\, dQ = \sum_i w_i \int_0^\infty \exp(-sQ) f_i(Q)\, dQ \tag{17}$$

Computing the Laplace transform of the distribution of quencher concentration is a convenient way to obtain an analytical expression for the fitting functions. Thus the pulse response function for any hypothetical distribution of quencher concentration can be immediately obtained from a table of Laplace transforms or with an analytical equation solver (e.g., MathCad, Mathematica). Following the analogy between the description of deterministic quencher distribution $f(Q)$ and probability density functions, we will compute fitting functions as Laplace transforms of several common probability density functions in the following section. Standard criteria for goodness of fit will be used to choose the most accurate approximation of quencher distribution. We will show that these fitting procedures result in accurate estimates of the parameters characterizing the distributions, and hence the mean and variance. However, it will be shown that it is practically impossible to discriminate between some fitting functions based on a goodness-of-fit criterion, although the moments of the distribution can be determined accurately. Therefore, in a subsequent section we will introduce an approximate scheme of determining the moments of the quencher distribution that makes no assumptions about a particular form of the distribution function. The histogram recovery method, based on a continuous representation of a histogram element (i.e., bin) will be proposed for the purpose of visualization of the underlying distribution.

PARAMETER IDENTIFICATION USING CONTINUOUS DISTRIBUTIONS

Unimodal distributions

In this section we will consider several examples of continuous distributions $f(Q)$, apply them to a simulated distribution of Q, and estimate the parameters of these distributions. We use the notation $2\delta = Q_{max} - Q_{min}$ and $Q_0 = (Q_{max} + Q_{min})/2$, or $Q_{min} = Q_0 - \delta$ and $Q_{max} = Q_0 + \delta$. Fig. 1 illustrates the distributions considered below.

Rectangular distribution

Information on the mean value and variance of quencher concentration in the emission volume can be obtained by using the model for a rectangular (or uniform) distribution, $f(Q)$ = constant, as a first approximation for many heterogeneous systems (Fig. 1). From the normalization condition (Eq. 8) we find for this simple case that

$$f(Q) = 1/2\delta \tag{18}$$

The simplest spatial distribution of Q corresponding to this distribution function is a linear one, e.g., $Q = Q_0 + Ax$ for $-a \le x \le a$, where A is the constant gradient in Q. In this case $\delta = Aa$. The first two moments of this distribution can be expressed, according to Eqs. 9 and 10, as

$$M = Q_0,\ \sigma^2 = \delta^2/3 \tag{19}$$

The fitting function for the rectangular distribution is

$$Y_R(t) = \exp(-(k_0 + k_q Q_0)t) \cdot \sinh(k_q \delta t)/k_q \delta t \tag{20}$$

This expression was recently presented by us (Zheng et al., 1996), and it contains the usual monoexponential term for mean quencher concentration, Q_0, multiplied by an additional term characterizing the concentration heterogeneity. For small values of the argument $\alpha = k_q \delta t$, $\sinh \alpha/\alpha \approx 1 + \alpha^2/6$, and, replacing δ with $3^{1/2}\sigma$ by using Eq. 19, we obtain the following approximation to Eq. 20:

$$Y_R(t) = \exp(-(k_0 + k_q M)t) \cdot [1 + (k_q \sigma t)^2/2] \tag{21}$$

For the case of a homogeneously distributed quencher, $\sigma = 0$, and the limit of $Y_R(t)$ gives the monoexponential decay (Eq. 6).

Normal distribution

The normal (Gaussian) distribution is a widely used statistical model for describing heterogeneity (Fig. 1):

$$f(Q) = (2\pi\sigma^2)^{-1/2}\exp(-(Q - M)^2/2\sigma^2) \quad (22)$$

With the normalization given in Eq. 22, the pulse response function can be obtained over the interval of concentration $(-\infty, \infty)$ rather than the interval $(0, \infty)$ used in Eqs. 8–12. Because $Q > 0$, the practical application of the following result for the normal distribution is restricted to cases where $M > 3\sigma$:

$$Y_N(t) = \exp(-(k_0 + k_qM)t)\exp((k_q\sigma t)^2/2) \quad (23)$$

Because of the choice of limits of integration, $Y_N(t)$ is not the Laplace transform of the corresponding distribution, in contrast with the other distributions considered in this paper; in particular, $Y_N \rightarrow \infty$ as $t \rightarrow \infty$. However, Eq. 21 can be used to fit experimental data within the time interval of practical interest.

Two-bar distribution

We consider a more complicated distribution to model asymmetrical distributions of quencher inside the emission volume: a simple asymmetrical two-bar distribution that consists of two adjacent rectangular distributions (Fig. 1). The distribution function, $f(Q)$, can be expressed in the form

$$f(Q) = \begin{cases} (0.5 - \phi)/\delta & \text{for } Q_0 - \delta \le Q < Q_0 \\ (0.5 + \phi)/\delta & \text{for } Q_0 \le Q \le Q_0 + \delta \end{cases} \quad (24)$$

The parameter ϕ characterizes the asymmetry of the model. The mean, variance, and skewness for this model are

$$M = Q_0 + \delta\phi,\ \sigma^2 = (\delta^2/3)(1 - 3\phi^2),\quad \gamma_1 = \mu_3/\sigma^3 \quad (25)$$

where $\mu_3 = -\delta^3\phi\,(1 - 4\phi^2)/2$. From Eq. 24, $-0.5 \le \phi \le 0.5$, thus $\gamma_1 < 0$ if $\phi > 0$, and $\gamma_1 > 0$ if $\phi < 0$. The fitting function for the two-bar distribution is

$$Y_{TB}(t) = \exp(-(k_0 + k_qQ_0)t) \cdot [\sinh(k_q\delta t) - 2\phi(\cosh(k_q\delta t) - 1)]/k_q\delta t \quad (26)$$

Gamma distribution

The gamma distribution is commonly used to describe asymmetrical (i.e., skewed) distributions of a nonnegative variable (Fig. 1):

$$f(Q) = [1/\beta^\alpha\Gamma(\alpha)]Q^{\alpha-1}\exp(-Q/\beta) \quad (27)$$

The first three moments expressed by Eqs. 9–11 are

$$M = \alpha\beta,\quad \sigma^2 = \alpha\beta^2,\quad \gamma_1 = 2\alpha^{-1/2} \quad (28)$$

The fitting function for the gamma distribution is

$$Y_G(t) = \exp(-k_0t)(1 + \beta k_qt)^{-\alpha} \quad (29)$$

Numerical procedures

MathCad (version 6.0, MathSoft) was used for analytical and numerical calculations, as well as simulation of phosphorescence emission in heterogeneous systems. The computer simulations of the phosphorescence decay time course assumed that the volume contained albumin-bound Pd-meso tetra (4-carboxyphenyl) porphine ($k_0 = 18.3 \cdot 10^{-4}\ \mu s^{-1}$, $k_q = 3.06 \cdot 10^{-4}\ mmHg^{-1}\ \mu s^{-1}$, and Q was expressed as PO_2 in mmHg; Zheng et al., 1996), which is used in the measurement of oxygen. Phosphorescence decay data were randomly generated by a Monte Carlo approach (Kalos and Whitlock, 1986) for rectangular, normal, two-bar, and gamma distributions (see Fig. 2 for examples). Briefly, the excitation/emission volume was represented as the sum of 200 spatial domains of equal size. For each domain, a value of PO_2 was randomly chosen from the distribution under consideration, and the phosphorescence lifetime associated with this domain was calculated from the Stern-Volmer equation (Eq. 7). Normalized phosphorescence decay curves from all of the domains were summed to produce an overall normalized decay curve for the whole volume.

Fitting of the simulated decay curves was performed with the Marquardt-Levenberg nonlinear least-squares algorithm, using the software Origin (version 3.5; MicroCal Software, Northampton, MA) with the four equations based on the continuous fitting functions (i.e., Eqs. 20, 23, 26, and 29). The monoexponential fit (Eq. 6) was also used for comparative analysis of the different approaches. Goodness of fit was assessed by calculating the mean sum of squares (MSS) for the fit of a normalized decay curve. MSS is defined as the sum of squares of the difference between the simulated decay curve, $Y_{sim}(t_i)$, and the fitting function, $Y_{fit}(t_i)$, divided by the number of degrees of freedom (df = number of data points − number of fitting parameters). The fitting procedure was terminated when MSS from two successive iterations differed by less than a tolerance value of 0.05. Results of fitting are expressed as mean (M) and standard deviation (σ). Random data generated from a rectangular distribution were used for evaluation of the accuracy and stability of distribution parameters as a function of heterogeneity of Q (e.g., PO_2). Similar random data generated from rectangular distributions were also used to study the stability and accuracy of the fitting models as a function of increasing the random noise level.

Results

The time course of phosphorescence caused by a short flash of excitation light could be described by Eqs. 20, 23, 26, or 29 for different distributions of quencher concentration. All of these equations are written in a similar form, as a product of the usual monoexponential decay for mean quencher concentration M times additional terms dependent on the heterogeneity of quencher concentration. We can recast the decay function from the product of a homogeneous term, $H(t)$, and a heterogeneous term, $R(t)$ (i.e., $Y(t) = H(t)\,R(t)$),

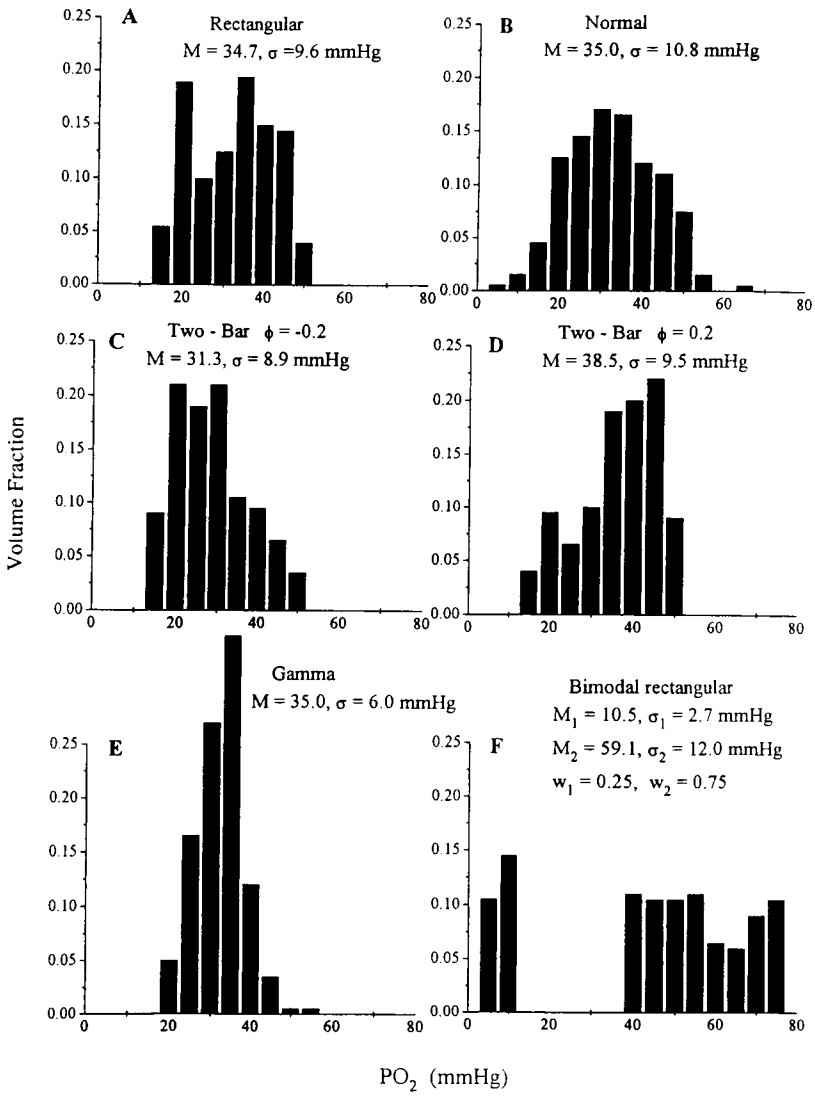

FIGURE 2 Computer-generated distributions of quencher concentration. Monte Carlo simulations were made by dividing the excitation volume into 200 regions of equal size and randomly drawing an oxygen tension (PO_2) from a specified continuous distribution with mean PO_2 of 35 mmHg and standard deviation of 10 mmHg.

to the sum of a homogeneous and a heterogeneous term by the following rearrangement:

$$Y(t) = H(t)R(t) = H(t) + H(t)[R(t) - 1] \qquad (30)$$

In this additive realization of $Y(t)$, the heterogeneous term is $H(t)\ [R(t) - 1]$. The relative contributions of the heterogeneous and homogeneous components of the decay signal can be expressed as their ratio: $R(t) - 1$. As a specific example, we can consider Eq. 20 for the rectangular distribution, where $R(t) = \sinh(k_q\delta t)/k_q\delta t$. Using the parameters above over a time interval 0–1 ms, $R(t) - 1$ increased from zero at $t = 0$, to 1.7 ($\sigma = 10$ mmHg) or 18 ($\sigma = 20$ mmHg) at 500 μs, up to 18 ($\sigma = 10$ mmHg) or 1900 ($\sigma = 20$ mmHg) at 1000 μs. Thus the contribution of the heterogeneous term increased strongly with σ and rapidly with time (see figure 3 *B* of Zheng et al., 1996). At these same time points for $M = 35$ mmHg, the homogeneous term decreased from unity to $2 \cdot 10^{-3}$, then to $4 \cdot 10^{-6}$, so that the data must have high-amplitude resolution and low noise level, over a time interval extending to approximately twice the exponential lifetime associated with the homogeneous term, to reveal the heterogeneity.

Table 1 presents the results of fitting the randomly generated decay curve obtained from a rectangular distribution with $M \approx 35$ mmHg and σ ranging from 0 to 20 mmHg, but because of the random nature of the simulation procedure, the resulting parameters exhibited small differences from the input values. Fitting was performed with the monoexponential (Eq. 6), rectangular, normal, two-bar, and gamma models of the pulse response functions. Fitting by the gamma model was unsatisfactory, presumably because of the intrinsic asymmetry of this distribution. Therefore, the results of the fits obtained by using the gamma distribution are not included in Table 1.

When the PO_2 domains were distributed with $\sigma = 0$, all of the fitting models except the gamma model returned a good estimate of M with the same fitting quality, and the continuous models returned a σ close to zero. The systematic error of estimation of mean PO_2 by the monoexponential model (underestimate) progressively grew up to −28%,

TABLE 1 Best-fit parameter values for increasing degree of heterogeneity

	Generated Parameter	Monoexponential	Rectangular	Normal	Two-bar	Taylor series
M	35.0	35.0	35.0	35.0	35.5	35.0
σ	0.0	—	0.21	0.24	0.87	0.001
MSS	—	6×10^{-8}	9×10^{-8}	6×10^{-8}	3×10^{-6}	6×10^{-8}
M	34.7	32.6	34.5	34.3	34.4	34.6
σ	9.6	—	9.9	9.3	9.8	10.6
MSS	—	2×10^{-5}	6×10^{-8}	2×10^{-7}	6×10^{-8}	3×10^{-7}
M	36.9	26.2	37.1	32.6	36.9	36.0
σ	20.3	—	20.9	18.5	20.4	22.4
MSS	—	7×10^{-4}	2×10^{-7}	6×10^{-5}	1×10^{-7}	2×10^{-4}

Phosphorescence decay curves were randomly generated from rectangular distributions. The Taylor series fitting function contains only the first two terms of the series. Mean (M) and standard deviation (σ) are given in mmHg. MSS is mean sum of squares for best fits by the different fitting functions.

as the heterogeneity, characterized by the coefficient of variation, CV = σ/M, increased from 0 to 55% (see Table 1). The rectangular and two-bar fitting models provided accurate evaluations of mean PO_2 and σ over a wide range of concentration heterogeneity, with a much better fitting quality estimated by the MSS (see Table 1). The normal model fitting equation (Eq. 23) also provided a good estimate for data generated by the rectangular distribution for $M > 3\sigma$.

To examine all four fitting models for stability in regard to distribution shape, simulated decay curves were generated randomly as described above, using rectangular, normal, gamma, and two two-bar distributions of left and right asymmetry (Fig. 2). The median PO_2 and standard deviation used for generating the pulse response function were M = 35 and σ = 10 mmHg. Results of simulated PO_2 distributions and results of their evaluation by fitting the associated phosphorescence decay curves with our models are shown in Table 2. Each fitting model was used to fit all of the generated data sets to compare parameter estimates among the different distributions. The evaluation of σ for symmetrical distributions by the gamma model was not very accurate (22–32% overestimate). The monoexponential fit was the poorest because it yielded the largest error in mean PO_2 (4–6% underestimate) and had the largest MSS. The continuous fitting models provided good accuracy for M and σ for all of the simulated distributions and gave MSSs that were two to three orders of magnitude smaller than that for the monoexponential model. The two-bar model generally gave the best results in terms of minimum MSS, and in addition, accurately reported the parameter of distribution asymmetry, ϕ (see Eqs. 24–26).

TABLE 2 Best-fit parameter values for different fitting functions and different generating distributions

Distribution	Parameter	Generated moments	Monoexponential	Rectangular	Normal	Gamma	Two-bar	Taylor series
Rectangular	M	34.7	32.6	34.5	34.3	35.4	34.4	34.6
	σ	9.6	—	9.9	9.3	12.7	9.8	10.6
	MSS	—	2×10^{-5}	6×10^{-8}	2×10^{-7}	3×10^{-6}	6×10^{-8}	3×10^{-7}
Normal	M	34.4	33.0	35.2	35.0	35.9	34.9	35.4
	σ	10.8	—	10.8	10.1	13.2	10.1	11.7
	MSS	—	2×10^{-5}	1×10^{-7}	1×10^{-7}	2×10^{-6}	8×10^{-8}	8×10^{-7}
Gamma	M	35.8	34.0	35.7	35.6	35.3	35.7	35.8
	σ	10.1	—	9.5	9.0	9.1	9.9	10.1
	MSS	—	1×10^{-5}	1×10^{-8}	1×10^{-7}	4×10^{-7}	2×10^{-8}	8×10^{-8}
Two-bar left asymmetry	M	31.3	29.8	31.2	31.1	31.2	31.3	31.3
	σ	8.9	—	8.3	7.9	8.6	9.5	8.8
	ϕ	−0.2	—	—	—	—	−0.23	—
	MSS	—	1×10^{-5}	1×10^{-7}	3×10^{-7}	1×10^{-7}	6×10^{-8}	7×10^{-8}
Two-bar right asymmetry	M	38.5	36.9	38.7	38.6	38.9	38.6	38.9
	σ	9.5	—	10.4	9.9	10.9	10.9	11.0
	ϕ	0.2	—	—	—	—	0.15	—
	MSS	—	1×10^{-5}	8×10^{-8}	7×10^{-8}	8×10^{-8}	5×10^{-8}	3×10^{-7}

Phosphorescence decay curves were generated by the distributions listed in the leftmost column. The resulting curves were fit by the functions listed in the table heading. The Taylor series fitting function contains only the first two terms of the series. Mean (M) and standard deviation (σ) are given in mmHg. MSS is mean sum of squares for best fits. ϕ is the asymmetry parameter for the two-bar model.

The simulation for the rectangular distribution of PO_2 was used to examine the stability of the best-fit parameters in the face of decreasing signal-to-noise ratio (SNR). In this paper, SNR is defined as the ratio of maximum signal amplitude to the peak-to-peak noise (noise for a single simulated event is equal to the total amplitude of noise times a random number on the symmetrical interval [−0.5, 0.5]). As shown in Fig. 3, the rectangular model (but not the monoexponential one) provided accurate and stable evaluations of mean PO_2 and σ when the SNR was greater than 13. Mean PO_2 can be determined with a small error for SNR down to 5, but after this limit the results become uncertain in all of the models, including the monoexponential model. Reducing the noise level below 1% (SNR > 100) cannot improve the fitting quality of the monoexponential model, but the MSS decreased by two orders of magnitude for the rectangular model (Fig. 3) under this condition.

DISTRIBUTION-FREE IDENTIFICATION OF MOMENTS

Results of the preceding section suggest that fitting with different distribution functions may lead to satisfactory evaluation of the mean and standard deviation (or variance) of simulated distributions. This suggested to us that it should be possible to evaluate the lower moments of a distribution without explicitly specifying the distribution function. To follow this argument, we recast Eq. 12 in the form

$$Y(t) = \exp(-(k_0 + k_q M)t)\int_0^\infty \exp(-k_q(Q - M)t)f(Q)\,dQ \tag{31}$$

The exponential term under the integral can be expanded in a Taylor series:

$$\exp(-k_q(Q - M)t) = 1 + \sum_{n=1}(-1)^n(k_q(Q - M)t)^n/n! \tag{32}$$

Substituting Eq. 32 into Eq. 31 and integrating, we obtain

$$Y_{TS}(t) = \exp(-(k_0 + k_q M)t)\left[1 + \sum_{n=2}(-1)^n\mu_n(k_q t)^n/n!\right]$$
$$= \exp[-(k_0 + k_q M)t][1 + \sigma^2 k_q^2 t^2/2 - \gamma_1\sigma^3 k_q^3 t^3/6$$
$$+ (\gamma_2 + 3)\sigma^4 k_q^4 t^4/24 + \ldots] \tag{33}$$

where the μ_n are the nth central moments of the distribution $f(Q)$ given by Eq. 11, γ_1 is the skewness coefficient, and γ_2 is the kurtosis. The first term of the series gives the monoexponential model, and the second term is an approximation of the rectangular model (Eq. 21). We used these first two terms in the series expansion to develop the fitting model based on this Taylor series expansion. The above formulation is analogous to calculations of the moment-generating function in probability theory (Beyer, 1968).

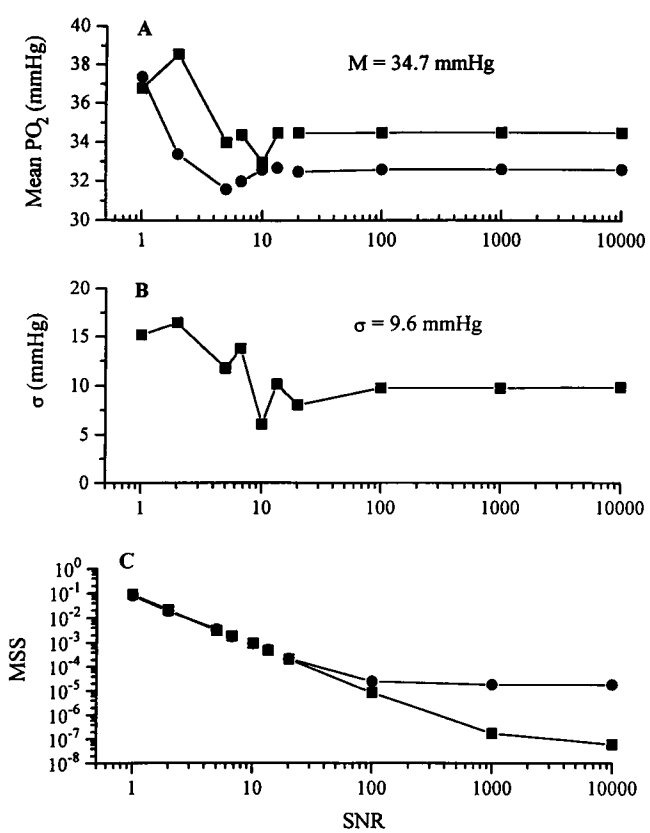

FIGURE 3 Results of fitting phosphorescence decay curves randomly generated according to a rectangular distribution (see Fig. 2) for different signal-to-noise ratios (SNRs). Fits were made to the rectangular (Eq. 20) and monoexponential (Eq. 6) fitting models. Mean (*top*) and standard deviation (*middle*) of PO_2 from computer-generated distribution are M = 34.7 mmHg and σ = 9.6 mmHg. (*Bottom*) MSS for different SNRs.

Results

The far right column of Tables 1 and 2 contains parameters evaluated from the simulated distributions, using the first two terms of Eq. 33 for comparison with the corresponding parameters in Tables 1 and 2. The Taylor series model is independent of the particular distribution and demonstrated a good ability to evaluate the first two moments of different PO_2 distributions. Attempts to find accurate estimates of higher moments were not successful.

MULTIMODAL DISTRIBUTIONS

All of the models worked out above describe heterogeneous systems in a single compartment. Under some experimental situations, the phosphorescence signals could arise from more than one heterogeneous compartment. For instance, in microcirculatory measurements of PO_2, the phosphorescence signals could originate from intravascular blood and perivascular tissue. To describe this situation, consider a volume V comprising N distinct compartments, each characterized by a volume V_i; quencher concentration Q_i, which

can vary within the compartment; and distribution function $f_i(Q_i)$, $i = 1, 2, \ldots, N$. We can express the integral in Eq. 12 as the sum of N integrals according to the property expressed in Eq. 17:

$$Y(t) = \sum_i w_i \int_{V_i} \exp(-(k_{0i} + k_{qi}Q_i)t) f_i(Q_i)\, dQ_i \quad (34)$$

Assuming that $f_i(Q_i)$ is a rectangular distribution for each compartment, we obtain from Eq. 34,

$$Y_{MR}(t) = \sum_i w_i \exp(-(k_0 + k_{qi}M_i)t) \cdot \sinh(k_{qi}\delta_i t)/k_{qi}\delta_i t \quad (35)$$

Similar calculations with the $f_i(Q_i)$ normal distributions yield

$$Y_{MN}(t) = \sum_i w_i \exp(-(k_0 + k_{qi}M_i)t)\exp((k_{qi}\sigma_i t)^2/2) \quad (36)$$

Each of these equations has $3N - 1$ fitting parameters, characterizing mean values M_i, heterogeneities σ_i or δ_i, and the weights w_i for each component. The case $N = 2$ (bimodal rectangular distribution in Fig. 1) is of particular importance for applications to oxygen measurements because the two compartments can represent intravascular and extravascular concentrations.

The distribution-free approach of the previous section (Eq. 33) can be extended to multicompartmental systems described by Eq. 33. Expanding each of the exponential functions in a Taylor series and integrating, we obtain

$$Y(t) = \sum_i w_i \exp(-(k_{0i} + k_{qi}M_i)t)\left[1 + \sum_{n=2}(-1)^n \mu_{ni}(k_{qi}t)^n/n!\right] \quad (37)$$

Simulation and fitting of bimodal distributions

To examine the ability of bimodal fitting functions (Eqs. 35 and 36 for $N = 2$) to resolve two separate distributions of quencher concentration on the basis of mixed decay curves, a bimodal rectangular distribution was generated randomly using the Monte Carlo simulation procedure described previously (see Fig. 2). The fitting results (Table 3) showed good resolution for mean values and standard deviations ($M_1 \pm \sigma_1$ and $M_2 \pm \sigma_2$) and the weight coefficient w_1 ($w_2 = 1 - w_1$) obtained with the bimodal rectangular model. Fitting this decay curve with the bimodal normal model returned results very close to those obtained with the bimodal rectangular model (no added noise): the first mode was 10.2 ± 2.4 mmHg, the second mode was 58.6 ± 12.9 mmHg, and w_1 was 0.26. The overall $M \pm \sigma$ for the bimodal distribution was 46.9 ± 21.4 mmHg and was estimated by the unimodal rectangular model (Eq. 20) as $M \pm \sigma$ = 48.0 ± 26.8 mmHg. The monoexponential fit gave M = 35.9 mmHg, a large underestimate of the weighted mean PO_2. The bimodal fitting models appear to be much more sensitive to the noise level than do the unimodal models that we have considered. Random noise as low as 2% of the maximum signal amplitude (SNR < 50) caused a large error in estimations of heterogeneity, whereas the mean values and weight coefficient were relatively accurate (see Table 3).

RECOVERY OF HISTOGRAMS OF QUENCHER DISTRIBUTION

In the present study we are interested in continuous distributions of Q. However, the analysis above is also valid for discrete distributions of Q. For example, if the volume V consists of N volumes V_i, $i = 1$ to N, $V = \Sigma_i V_i$, and in each of these volumes the quencher concentration is uniform, $Q = Q_i$ = constant, then

$$f(Q) = \sum_i w_i \delta(Q - Q_i) \quad (38)$$

where $\delta(Q)$ is the Dirac delta function and the weighting factors were defined earlier (Provencher, 1976a,b). Thus the integral in Eq. 12 becomes

$$Y_D(t) = \sum_i w_i \exp(-(k_0 + k_q Q_i)t) \quad (39)$$

The mathematical problem in this case is to determine the parameters w_i and Q_i. For uniformly spaced and fixed Q_i, only the set of $n - 1$ values of w_i has to be determined in the ESM and MEM approaches (James and Ware, 1986; Livesey and Brochon, 1987) and in the quadratic programming algorithm (Vinogradov and Wilson, 1994). Because of the large number (up to 200) of monoexponentials in the fitting function used in these studies, the calculation time was substantial.

TABLE 3 Effect of noise on fitting by bimodal rectangular model

Parameters	Generated moments	SNR = 1000	SNR = 100	SNR = 50	SNR = 20	SNR = 10
M_1	10.5	9.9	9.6	11.3	11.4	10.6
M_2	59.1	58.5	57.9	57.1	53.1	53.7
σ_1	2.8	2.1	2.7	5.6	5.8	6.4
σ_2	12.0	13.5	15.2	15.2	20.1	25.8
w_1	0.25	0.26	0.28	0.26	0.24	0.26
MSS	—	6×10^{-9}	8×10^{-6}	3×10^{-5}	9×10^{-4}	1×10^{-3}

Phosphorescence decay curves were generated for the bimodal distribution using the values listed for mean (M_1 and M_2) and standard deviation (σ_1 and σ_2) of PO_2 (in mmHg) and weight (w_1) of first mode. MSS is mean sum of squares of the best fit. Signal-to-noise ratio (SNR) decreases from left to right.

However, the calculations of quencher distribution can be significantly simplified, with a corresponding reduction in computation time, if we represent the quencher concentration by a histogram containing a relatively small number of bins (N = 5–10) and consider each bin to represent a rectangular distribution of quencher of width 2δ and mean value Q_i, comprising a fraction, w_i, of the heterogeneous volume. According to Eq. 20, the contribution of bin i to the total normalized phosphorescence decay signal is y_i, so that

$$y_i(t) = w_i \exp(-k_0 t)\exp(-k_q Q_i t)\sinh(k_q \delta t)/k_q \delta t \qquad (40)$$

Because $Y(t) = \Sigma_i y_i(t)$ and $\Sigma_i w_i = 1$, we can define a new transformed decay function, $Y^*(t)$, so that

$$Y^*(t) = Y(t)[\exp(k_0 t)k_q \delta t/\sinh(k_q \delta t)] = \sum_i w_i \exp(-k_q Q_i t) \qquad (41)$$

Thus the original decay curve, $Y(t)$, multiplied by the known function in brackets, is equal to the sum of monoexponentials of known equidistant Q_i, with unknown weighting coefficients. Experimental data for the normalized decay curve, $Y(t)$, after the above transformation, can be fit by Eq. 41, yielding best-fit values for the w_i, with the constraint $w_i \geq 0$.

Equation 41 can be reparameterized using the definition $Q_i = (2i - 1)\ \delta$, $i = 1, N$. The transformed decay function $Y^{**}(X)$, where $X(t) = \exp(-2k_q \delta t)$, can then be defined as

$$Y^{**}(X) = Y(t)[\exp(k_0 t)2k_q \delta t/(\exp(2k_q \delta t) - 1)] = \sum_i w_i X^i \qquad (42)$$

Thus, after the data are transformed according to Eq. 42, they can be fit using a polynomial fitting procedure for the function $Y^{**}(X)$ to recover the weight factors, w_i. The first two central moments of the distribution obtained in this way can be calculated with the formulae

$$M = \sum_i w_i Q_i, \quad \sigma^2 = \sum_i w_i Q_i^2 - M^2 \qquad (43)$$

Numerical procedures

A histogram of eight bins (bins centered at Q_i = 5, 15, . . . , 75 mmHg; δ = 5 mmHg) was used to recover the computer-generated distributions of PO_2 according to Eq. 41. The w_i were determined by the same nonlinear least-squares fitting software described above, with the constraint that $w_i \geq 0$. The plot of w_i versus Q_i is a histogram of the quencher concentration.

Results

The ability of the fitting procedure (Eq. 41) to recover the histogram representing a normal (Gaussian) distribution of PO_2 is shown in Fig. 4. The quality of the recovered histogram depends significantly on the SNR. For SNR > 20, the histograms of generated and fit data are not significantly different ($p > 0.05$) by a Kolmogorov-Smirnov test (Zar, 1984), and the fits yield accurate estimates of M and σ. When the SNR decreases to 20, however, the estimate of mean PO_2 is low by 13% and the error in σ is almost 30%. This gives an example of the histogram recovery procedure for the particular case of a normal (Gaussian) distribution. The general conditions for which the recovery of a histogram is possible with acceptable accuracy should be investigated further.

DISCUSSION

We have previously reported that phosphorescence decay curves obtained from in vivo and in vitro heterogeneous systems could not be satisfactorily described with a monoexponential function (Zheng et al., 1996). The continuous distribution approach yields fitting functions that provide a good fit of the pulse response function of phosphorescence decay in a heterogeneous volume and explains it in generally accepted statistical terms. Although these models describe hypothetical distributions of quencher that have relatively simple analytical expressions, they can be applied as fitting models and diagnostic tools for the analysis of actual experimental data. Thus these models can be applied 1) to determine the mean concentration of quencher and evaluate its variability; 2) to distinguish between homogeneous and heterogeneous as well as unimodal and bimodal distributions; and 3) to determine the degree of asymmetry of a distribution.

The analysis of phosphorescence decay curves in terms of continuous distributions is pertinent to heterogeneous systems produced by convective and diffusive gradients. Compared to a monoexponential fit, this approach minimizes the systematic errors by weighting the volume fractions corresponding to different quencher concentrations. Use of a monoexponential fit to recover mean PO_2 in a volume with a large PO_2 gradient (e.g., perivascular tissue) can lead to a substantial underestimation of mean PO_2.

The best evaluation of σ for an unknown distribution can be obtained from the fitting function that provides the best goodness of fit. One can approximate the real distribution inside the emission volume by selecting the fitting model with the least MSS. However, if the distribution function, $f(Q)$, is known, the corresponding fitting function can be obtained using Eq. 12. If the size of the emission volume is large compared with the distance over which the gradient in quencher concentration exists, a number of statistical distributions could be used. However, the possible distribution of quencher within the emission volume should be estimated from an appropriate physical model for $f(Q)$, taking into account the geometric and kinetic parameters of the system under study. For example, one could formulate a model of oxygen distribution in microvessels by including the known flow behavior of red blood cells and the hemoglobin-oxygen binding and release kinetics and convert it to the corresponding phosphorescence decay time course using tables of Laplace transforms or integration of Eq. 12.

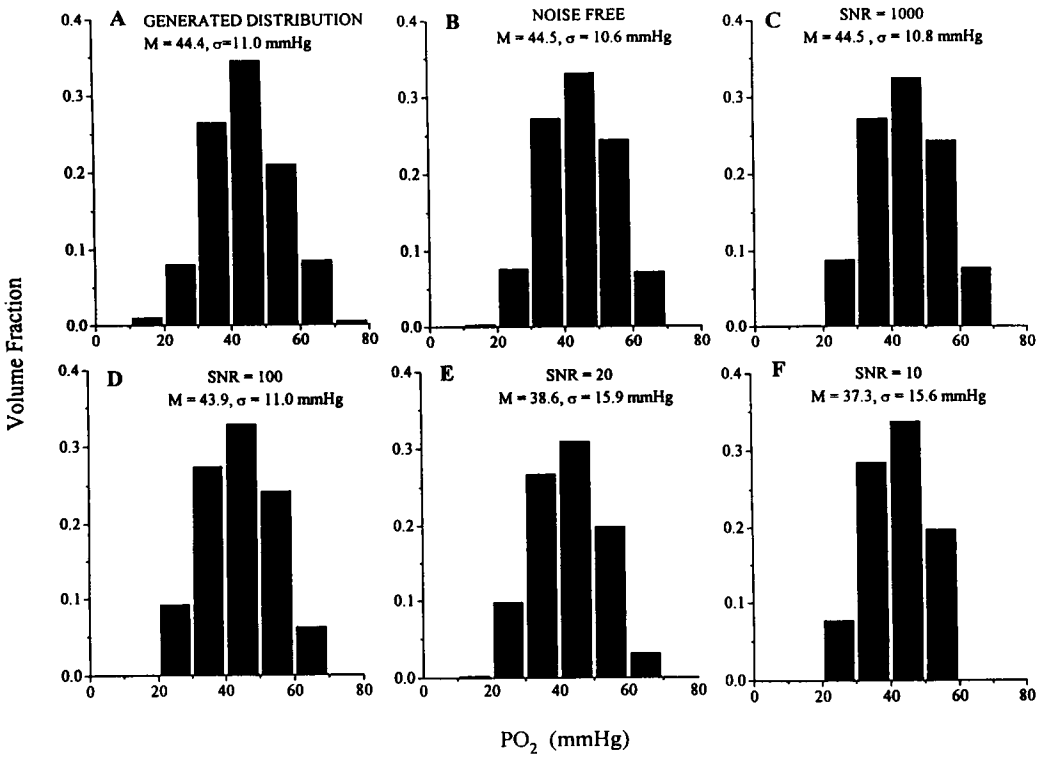

FIGURE 4 Effect of altered signal-to-noise ratio (SNR) on ability of histogram fitting procedure to recover original computer-generated Gaussian distribution of PO_2. For SNR > 100, recovery of both M and σ is quite accurate. Results of a Kolmogorov-Smirnov test comparing the original distribution with the histogram fits for decreasing SNR show that the fitted histograms are not significantly different from the original distribution ($p > 0.05$) for SNR > 20.

The most valuable feature of the continuous models is their stability and accuracy with increasing heterogeneity. A monoexponential fit yields significant systematic error that underestimates the mean values by up to one-third when the CV exceeds 50% (Table 1). Generally, the fitting models returned accurate estimates for M and σ independent of the particular distribution of quencher concentration. The Taylor series model demonstrated that reliable values for the first two moments of a distribution could be obtained without specific knowledge of its shape.

The histogram recovery procedure, based on the continuous representation of concentration distribution as a set of several rectangular distributions, needed smaller computer resources than deconvolution of a set of 200 monoexponential compartments (Vinogradov and Wilson, 1994). A comparison of Eqs. 39 and 40, which represent the discrete and continuous approaches, respectively, shows that, for the same set of equidistant Q_i values separated by 2δ, they differ by the "heterogeneous factor" of Eq. 20 (i.e., $\sinh(k_q\delta t)/k_q\delta t$). This factor can be used as a quantitative index of the difference between decay curves from the same quencher concentration distribution represented by the discrete (ESM) approach of Eq. 39 and by a continuous histogram (i.e., $\Sigma_i y_i(t)$ from Eq. 40). For the values of k_0 and k_q used in our simulations, we can compare, for instance, the normalized signal difference at 1 ms after the excitation flash (i.e., $\sinh(k_q\delta t)/k_q\delta t - 1$). For $\delta = 1$ mmHg, the difference is negligible at 1.6%; for $\delta = 2$ mmHg it is 6.4%; and for $\delta = 5$ mmHg the discrete representation of the quencher distribution (as in Eq. 39) leads to a difference of 44%. That is why, to achieve adequate resolution of the distribution in quencher concentration, the ESM and MEM approaches require such a large number of parameters to diminish the error in representing a continuous distribution by a discrete sum of monoexponentials, whereas the histogram approach, based on a continuous representation of the distribution, can achieve the same resolution with a significantly smaller number of parameters.

The reparameterization of fitting functions is a useful and generally accepted procedure in nonlinear fitting (Motulsky and Ransnas, 1987). However, the transformation function can amplify the noise in the tail of the decay curve and bias the estimated parameters. Evaluation of the transformation factor in Eq. 41 for the values of k_0 and k_q used in our simulation showed that it increased from 1 (at $t = 0$) up to 4.3 (at $t = 1$ ms) for $\delta = 5$ mmHg; but, for δ greater than 8–10 mmHg, the factor decreased below 1, diminishing the influence of noise. This threshold level for δ in the transformation factor of Eq. 42 is even lower, 4–5 mmHg, allowing a smaller bin size and better resolution of the quencher distribution. Estimates of this kind should be carried out to optimize the bin width of the fitting function for the histogram recovery procedure. The fitting procedure for this histogram representation of the quencher distribu-

tion is significantly faster than that described by Vinogradov and Wilson (1994). The histogram approach may thus provide an opportunity for the on-line determination of quencher distribution.

The accuracy of parameter estimates depends on the quality of the photometric signals. The contribution of the heterogeneous component of the phosphorescence signal is small in the initial part of the decay curve, but significant in the later part of the curve, where the signal amplitude and signal-to-noise ratio become smaller. The influence of terms related to the asymmetry of the distribution is quite small in the early part of the decay curve. To extract the most complete and accurate information from a decay curve, it is therefore important to reduce the noise level and to accurately determine the baseline. A common approach to reducing the noise level is to average sequential decay curves. However, there is no way to distinguish spatial and temporal heterogeneity from the resulting decay curve. To obtain information on the spatial distribution of quencher in the unsteady state (e.g., capillary blood flow), individual decay curves should be processed. This requires that efforts be made to improve the signal-to-noise ratio.

The actual experimental signal from a phosphorimeter is influenced by characteristics of the data acquisition system, in addition to the true phosphorescence decay (Ware et al., 1973). This instrumental contribution can be determined empirically by measuring the response of the system to an excitation flash in the absence of phosphor. For instance, if the detected phosphorescence decay signal contains remnants of the flash whose intensity decays more rapidly than the true phosphorescence decay (apparent short lifetime), this would be interpreted in the analysis as a contribution from a region with high quencher concentration. Each instrumental artifact, such as the excitation flash decay and electronic filtering of the photomultiplier signal, has a characteristic "lifetime." The location (i.e., range of Q) of the artifact can be calculated by noting the correspondence between the apparent "lifetime" and quencher concentration as given by the Stern-Volmer equation (Eq. 7). Bins can be placed in the histogram to specifically cover the range of Q associated with the artifact(s). To the extent possible, the instrumentation should be adjusted to produce apparent "lifetimes" that correspond to quencher concentrations that exceed any realistic values in the sample under study. An advantage of the histogram algorithm is that instrumental artifacts affecting the phosphorescence decay curve can be taken into account by displaying the histogram representing the weights of various quencher concentrations. Any bins with nonzero contributions at quencher concentrations above a realistic maximum can be related to some feature of the detection/data acquisition system. Contributions of artifacts can thus be isolated and removed from the histogram, so that the true distribution of quencher concentration can be revealed and studied.

A practical procedure for analyzing a phosphorescence decay curve produced by an unknown distribution of quencher consists of the following steps. First, the decay curve can be analyzed crudely by using the rectangular fitting model to generate initial estimates for M and σ. If σ is large (i.e., $\sigma \approx M$), this could indicate that the distribution in quencher concentration is not unimodal. The decay curve should then be fit by using the bimodal fitting model to get estimates of M and σ for the two modes. The next step is to fit the decay curve according to the histogram algorithm using a small number of bins (i.e., 5–8) that cover the full range of quencher concentration revealed by the bimodal analysis. As described above, instrumental artifacts can be identified and eliminated or minimized in the contributing instrumentation, but they can also be dealt with during the analysis phase by removing the part of the histogram that corresponds to the artifact(s). Once this has been accomplished, the histogram can be rescaled to display concentration regions where $w_i \neq 0$. By using the histogram algorithm, a more complete and accurate description of the distribution of quencher concentration within a given sample volume can be obtained than is possible with the simple monoexponential fitting approach.

This work was supported in part by grant HL 18292 from the National Heart, Lung and Blood Institute and by a grant-in-aid from the American Heart Association, Virginia Affiliate.

REFERENCES

Alcala, J. R., E. Cratton, and F. G. Prendergast. 1987. Resolvability of fluorescence lifetime distributions using phase fluorometry. *Biophys. J.* 51:587–596.

Bevington, P. R. 1969. Data Reduction and Error Analysis for the Physical Sciences. McGraw-Hill, New York.

Beyer, W. H. 1968. CRC Handbook of Tables for Probability and Statistics. CRC Press, Boca Raton, FL. 16.

Boas, M. L. 1983. Mathematical Methods in the Physical Sciences. John Wiley and Sons, New York.

Ellsworth, M. L. and R. N. Pittman. 1986. Evaluation of photometric methods for quantifying convective mass transport in microvessels. *Am. J. Physiol.* 251:H869–H879.

Ellsworth, M. L., A. S. Popel, and R. N. Pittman. 1988. Assessment and impact of heterogeneities of convective oxygen transport parameters in capillaries of striated muscle: experimental and theoretical. *Microvasc. Res.* 35:341–367.

Englander, S. W., D. B. Calhoun, and J. J. Englander. 1987. Biochemistry without oxygen. *Anal. Biochem.* 161:300–306.

Federspiel, W. J., and A. S. Popel. 1986. A theoretical analysis of the effect of the particulate nature of blood on oxygen release in capillaries. *Microvasc. Res.* 32:164–189.

Gardner, D. G., J. C. Gardner, G. Laush, and W. W. Menke. 1959. Methods for analysis of multicomponent exponential decay curves. *J. Chem. Phys.* 31:978–986.

Isenberg, I., and R. D. Dyson. 1969. The analysis of fluorescence decay by a method of moments. *Biophys. J.* 9:1337–1350.

James, D. R., Y. S. Liu, P. De Maio, and W. R. Ware. 1985. Distributions of fluorescence lifetimes: consequences for the photophysics of molecules adsorbed on surfaces. *Chem. Phys. Lett.* 120:460–465.

James, D. R., and W. R. Ware. 1985. A fallacy in the interpretation of fluorescence decay parameters. *Chem. Phys. Lett.* 120:455–459.

James, D. R., and W. R. Ware. 1986. Recovery of underlying distributions of lifetimes from fluorescence decay data. *Chem. Phys. Lett.* 126:7–11.

Kalos, M. H., and P. A. Whitlock. 1986. Monte Carlo Methods, Vol. 1, Basics. John Wiley, New York.

Kerger, H., D. J. Saltzman, M. D. Menger, K. Messmer, and M. Intaglietta. 1996. Systemic and subcutaneous microvascular PO_2 dissociation during hemorrhagic shock in conscious hamsters. *Am. J. Physiol.* 270: H827–H836.

Kerger, H., I. P. Torres Filho, M. Rivas, R. M. Winslow, and M. Intaglietta. 1995. Systemic and subcutaneous microvascular oxygen tension in conscious Syrian golden hamsters. *Am. J. Physiol.* 268:H802–H810.

Kuo, L., and R. N. Pittman. 1988. Effect of hemodilution on oxygen transport in arteriolar networks of hamster striated muscle. *Am. J. Physiol.* 254:H331–H339.

Kuo, L., and R. N. Pittman. 1990. Influence of hemoconcentration on arteriolar oxygen transport in hamster striated muscle. *Am. J. Physiol.* 259:H1694–H1702.

Lakowicz, J. R., G. Laczko, H. Cherek, E. Cratton, and M. Limkeman. 1984. Analysis of fluorescence decay kinetics from variable-frequency phase shift and modulation data. *Biophys. J.* 46:463–477.

Livesey, A. K., and J. C. Brochon. 1987. Analyzing the distribution of decay constants in pulse-fluorometry using the maximum entropy method. *Biophys. J.* 52:693–706.

Morse, P. M., and H. Feshbach. 1953. Methods of Theoretical Physics. McGraw-Hill, New York. 925–949.

Motulsky, H. J., and L. A. Ransnas. 1987. Fitting curves to data using nonlinear regression: a practical and nonmathematical review. *FASEB J.* 1:365–374.

Popel, A. S. 1989. Theory of oxygen transport to tissue. *Crit. Rev. Biomed. Eng.* 17:257–321.

Provencher, S. W. 1976a. A Fourier method for the analysis of exponential decay curves. *Biophys. J.* 16:27–41.

Provencher, S. W. 1976b. An eigenfunction expansion method for the analysis of exponential decay curves. *J. Chem. Phys.* 64:2772–2777.

Shonat, R. D., K. N. Richmond, and P. C. Johnson. 1995. Phosphorescence quenching and the microcirculation: an automated, multipoint oxygen tension measuring instrument. *Rev. Sci. Instrum.* 66:5075–5084.

Shonat, R. D., D. F. Wilson, C. E. Riva, and M. Pawlowski. 1992. Oxygen distribution in the retinal and choroidal vessels of the cat as measured by a new phosphorescence imaging method. *Appl. Optics.* 31: 3711–3718.

Siemiarczuk, A., B. D. Wagner, and W. R. Ware. 1990. Comparison of the maximum entropy and exponential series methods for the recovery of distributions of lifetimes from fluorescence lifetime data. *J. Phys. Chem.* 94:1661–1666.

Siemiarczuk, A., W. R. Ware, and Y. S. Liu. 1993. A novel method for determining size distribution in polydisperse micelle systems based on the recovery of fluorescence lifetime distributions. *J. Phys. Chem.* 97: 8082–8091.

Swain, D. P., and R. N. Pittman. 1989. Oxygen exchange in the microcirculation of hamster retractor muscle. *Am. J. Physiol.* 256: H247–H255.

Torres Filho, I. P., and M. Intaglietta. 1993. Microvessel pO_2 measurements by phosphorescence decay method. *Am. J. Physiol.* 265: H1434–H1438.

Torres Filho, I. P., H. Kerger, and M. Intaglietta. 1996. pO_2 measurements in arteriolar networks. *Microvasc. Res.* 51:202–212.

Torres Filho, I. P., M. Leunig, F. Yuan, M. Intaglietta, and R. K. Jain. 1994. Noninvasive measurement of microvascular and interstitial oxygen profiles in a human tumor in SCID mice. *Proc. Natl. Acad. Sci. USA.* 91:2081–2085.

Vanderkooi, J. M., G. Maniara, T. J. Green, and D. F. Wilson. 1987. An optical method for measurement of dioxygen concentration based upon quenching of phosphorescence. *J. Biol. Chem.* 252:5476–5482.

Vinogradov, S. A., L-W. Lo, W. T. Jenkins, S. M. Evans, C. Koch, and D. F. Wilson. 1996. Noninvasive imaging of the distribution in oxygen in tissue in vivo using near-infrared phosphors. *Biophys. J.* 70:1609–1617.

Vinogradov, S. A., and D. F. Wilson. 1994. Phosphorescence lifetime analysis with a quadratic programming algorithm for determining quencher distribution in heterogeneous systems. *Biophys. J.* 67: 2048–2059.

Ware, W. R. 1991. Recovery of fluorescence lifetime distributions in heterogeneous systems. *In* Photochemistry in Organized and Constrained Media. V. Ramamurthy, editor. VCH Publishers, New York. 563–602.

Ware, W. R., L. J. Doemeny, and T. L. Nemzek. 1973. Deconvolution of fluorescence and phosphorescence decay curves. A least square method. *J. Chem. Phys.* 77:2038–2048.

Wilson, D. F., A. Pastuszko, J. E. DiDiacomo, M. Pawlowski, R. Schneiderman, and M. Delivoria-Papadopoulos. 1991. Effect of hyperventilation on oxygenation of the brain cortex of newborn piglets. *J. Appl. Physiol.* 70:2691–2696.

Zar, J. H. 1984. Biostatistical Analysis. Prentice-Hall, Englewood Cliffs, NJ.

Zheng, L., A. S. Golub, and R. N. Pittman. 1996. Determination of PO_2 and its heterogeneity in single capillaries. *Am. J. Physiol.* 271:H365–H372.